Measurements and Retrievals from a New 183-GHz Water Vapor Radiometer in the Arctic

Maria P. Cadeddu[1], James C. Liljegren[1], and Andrew Pazmany[2]

***Abstract*— A new G-band (183.31-GHz) vapor radiometer (GVR) developed and built by ProSensing Inc. was deployed in Barrow, Alaska, in April 2005. The radiometer is part of a suite of instruments maintained by the Atmospheric Radiation Measurement (ARM) Program. The instrument measures brightness temperatures from four double sideband channels centered at ±1, ±3, ±7, and ±14 GHz from the 183.31-GHz water vapor line. Atmospheric emission in this spectral region is primarily due to water vapor, with some influence from liquid water. The GVR will remain in Barrow through the winter and will collect data for several months in a dry and cold environment, when its sensitivity is best.**

In this paper, data collected in November 2005, December 2005, and January 2006 are shown. Measurements are compared with simulations obtained by using a radiative transfer model. We show that the measurements agree well with model simulations. Precipitable water vapor (PWV) and liquid water path (LWP) are retrieved with a nonlinear physical algorithm, and results are compared with those from the co-located dual-channel microwave radiometer (MWR) and radiosondes. Retrieval errors are estimated to be better than 5% for precipitable water vapor and of the order of 0.006 mm for LWP.

***Index Terms*—Microwave radiometry, remote sensing, water vapor retrieval.**

I. INTRODUCTION

THE GVR is part of a suite of instruments deployed by the ARM Program to improve observations of low amounts of PWV (< 5 mm) and low amounts of liquid water (LWP < 50 g/m^2). Water vapor, as one of the most variable atmospheric constituent, plays a crucial role in the analysis of local weather patterns, as well as in the validation of global climate models. Accurate water vapor measurements are essential in assessing the performance of clear-sky radiative flux models. PWV retrieval errors achieved with traditional linear statistical retrievals from microwave measurements are around 0.4 mm. Microwave radiometry is also an established method to retrieve accurate liquid water path that is necessary to the study of the role of clouds in the Earth radiation balance. LWP retrieval errors are around 0.02 mm (or 20 g/m^2) however, as shown in [1], a large percentage of clouds have LWP of less than 100 g/m^2. Traditional ground-based measurements employ two or more channels located in the spectral region of water vapor absorption at 22 GHz and one channel in the liquid absorption region around 30 GHz. In particular, the ARM Program has been operating for several years a two-channel microwave radiometer, the MWR, with frequencies at 23.8 and 31.4 GHz. During the cold Arctic winter, the amount of PWV is often less than 3 mm and clouds with LWP of less than 50 g/m^2 are common. In these conditions the dual-channel MWR is operating at the limit of its capabilities with a very low signal-to-noise ratio. Several authors, [1], [2], and [3] to mention just some examples, have analyzed the origin of uncertainties in MWR retrieval. Besides calibration issues and the effect of measurement noise, uncertainty in the liquid water retrieval can be attributed to the modeling of the dry opacity term and to the cloud liquid absorption coefficient. One result of these uncertainties is the fact that the MWR can retrieve LWP significantly higher than zero, when the sky is clear (i.e. there are no liquid clouds).

Because of its increased sensitivity to water vapor the 183.31-GHz absorption line can help improve water vapor retrievals during the dry Arctic winter. However, the dependence of brightness temperatures on precipitable water vapor and liquid water is linear only in a limited region, and a nonlinear retrieval algorithm is needed. An additional layer of complexity is added by the fact that the radiometer response saturates at a PWV of ~ 5 mm [4] for the most sensitive channels. The absorption line centered at 183.3 GHz has been extensively used from satellites [5] and aircraft [6], however very few measurements ([7], [4]) have been reported from the ground. The GVR has been operating in Barrow, Alaska for one year and is the first ground-based radiometer operating at 183.3 GHz permanently deployed at an Arctic location with the purpose of improving PWV and LWP retrievals.

The purpose of this paper is to analyze the data from the GVR and to assess the capability of this instrument to supplement the MWR retrievals in very dry conditions. The considerable length of time during which the radiometer has been operating has been very important to assess the stability of the instrument and the quality of the calibration. The paper

Manuscript received April ***, 2006. This work was supported by the Climate Change Research Division, U.S. Department of Energy, Office of Science, Office of Biological and Environmental Research, under contract W-31-109-Eng-38, as part of the ARM Program. Argonne National Laboratory is operated by the University of Chicago for the U. S. Department of Energy.

M. P. Cadeddu is with Argonne National Laboratory, Argonne, IL 60439 USA (phone: 630-252-7408; e-mail: mcadeddu@anl.gov).

J. C. Liljegren, is with Argonne National Laboratory, Argonne, IL 60439 USA (e-mail: jcliljegren@anl.gov).

A. Pazmany is with Prosensing, Inc. Amherst, MA 01002 USA, (e-mail: pazmany@prosensing.com).

This work was supported by the Climate Change Research Division, U.S. Department of Energy, Office of Science, Office of Biological and Environmental Research, under contract W-31-109-Eng-38, as part of the ARM Program. Argonne National Laboratory is operated by the University of Chicago for the U. S. Department of Energy.

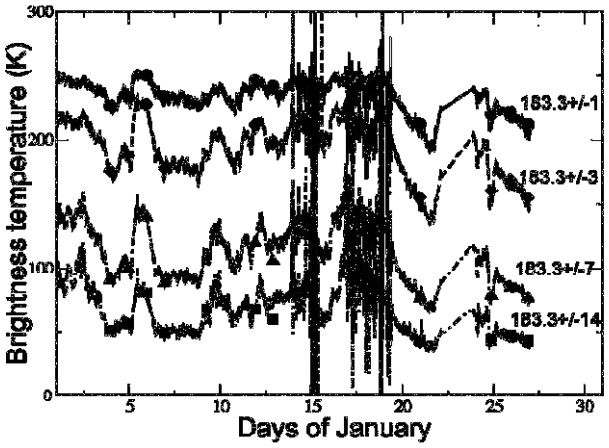

Fig. 1. Brightness temperatures measured by the GVR during the month of January. Model computations during clear-sky conditions are shown as circles, diamonds, triangles and squares. High noise level between day 15 and 20 are due to thermal instability of the instrument.

is organized as follows: In section II is given a brief description of the instrument. In section III and IV measured brightness temperatures are compared to model computations and their sensitivity to water vapor and cloud liquid water are assessed. The retrieval algorithm is described in section V and, in section VI, PWV and LWP retrievals are discussed, retrieval errors are theoretically quantified and their dependence on the amount of PWV is shown. The large dataset has also provided us with the opportunity to carry an extensive comparison with retrievals from the MWR and Vaisala R90 radiosonde under a range of water vapor conditions. Specific attention is devoted in section VII to the analysis of retrieved LWP under clear sky conditions and its comparison with the MWR. A brief summary of results is given in the conclusive section. We conclude that PWV retrievals from the GVR can achieve an accuracy of better than 5% for PWV amounts of less than 8 mm. Expected clear-sky retrievals of LWP have standard deviations of less than 0.002 mm.

II. The Instrument

The GVR, developed and built by ProSensing Inc. (http://www.prosensing.com) [8], measures brightness temperatures from four double sideband channels centered at ± 1, ± 3, ± 7, and ± 14 GHz from the 183.31-GHz water vapor line. Atmospheric emission in this spectral region is primarily due to water vapor, with some influence from liquid water. The 183.3 ± 14 GHz channel is particularly sensitive to the presence of liquid water. Bandwidths for the four channels are 0.4, 1.0, 1.4, and 2.0 GHz. The radiometer uses a hot (~ 330 K) and warm (290 K) calibration target. ProSensing expects a calibration accuracy of better than 1 K. The GVR started collecting data successfully immediately after deployment. On the first day of collection, it was found that a radar operated by the U.S. Air Force in the vicinity of the radiometer was causing a strong interference with the 183.3 ± 1 GHz channel. To eliminate this effect, a conservative filter was applied to all frequencies. Apart from intermittent high noise due to thermal instability, instrument operations have been stable. For the purpose of this analysis, data during cold days (surface temperatures of less than 255 K) were chosen in order to avoid excessive noise.

III. Measurement-Model Comparison

The GVR has been operating at the North Slope of Alaska (NSA) site since April 2005. Although operations have been continuous, this data analysis will cover only data collected during the cold winter months, when low-humidity conditions prevail. A time series of data collected in January 2006 is shown in Fig. 1. Some periods of enhanced noise are visible on days 13-19. Temperature instability in the radiometer was responsible for the noisy data. Additional periods of enhanced noise (not shown) are present during the months of November and December.

Simulated brightness temperatures shown in Fig. 1 are computed by using the radiative transfer code MonoRTM [9] with the HITRAN database line parameters [10] and the so-called CKD 2.4 continuum [11]. Only radiosonde data collected during clear conditions were used to compute brightness temperatures. The clear-sky screening dramatically decreased the amount of data available for the comparison. Radiosondes (Vaisala RS90) are launched at the NSA site once a day, five days a week. The original number of radiosondes available was 55 (17 in November, 18 in December, and 20 in January). Once data were screened for clouds, only 30 cases were left (10 in November, 11 in December, and 9 in January). The agreement between measurements and observations is satisfactory at all frequencies. Large discrepancies between measured and modeled brightness temperatures at similar frequencies were recently reported in [4]. The improved agreement observed in this comparison can be attributed, at least in part, to improved radiosonde measurements. Mean and standard deviation of measurements-minus-model computations is displayed in Table 1. A scatter plot of measured and modeled brightness temperature is shown in Figure 2. From this comparison it appears that the model is in acceptable agreement with the measurements. The larger discrepancies are observed at 183.3 ± 1 GHz where the model overestimates the measurements of about 4 K. The overestimation has a slight dependence on the brightness temperature itself.

TABLE I
MEAN AND STANDARD DEVIATION OF MEASURED-MINUS-MODELED BRIGHTNESS TEMPERATURES FOR THE MONTHS OF NOVEMBER, DECEMBER, AND JANUARY AT THE NSA (N=31).

Frequency GHz	Mean K	Standard deviation K
183.3 ± 1	-3.81	2.03
183.3 ± 3	-2.77	2.08
183.3 ±7	3.03	2.90
183.3 ± 14	1.49	3.87

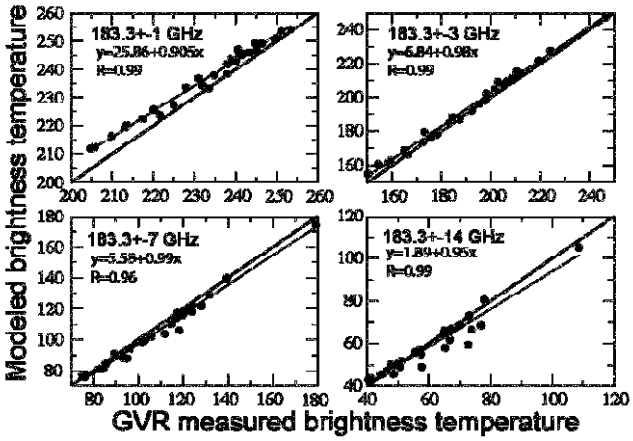

Fig. 2. Scatter-plot of clear-sky measured (x-axis) and modeled (y-axis) brightness temperatures. Data were collected during November, December and January (N=31)

IV. Sensitivity to PWV and LWP

The sensitivity of the GVR channels to the presence of water vapor is much stronger than the 22 GHz water vapor line [4]. In Figure 3 the dependence of GVR-measured brightness temperatures on PWV is shown. The PWV is retrieved from the MWR. The circles, diamonds, triangles and squares, are model computations from one year of radiosonde data. Fig. 3 shows the non-linear response of the GVR to water vapor as well as the saturation of the channels close to the line center. These results are consistent with those of [4] who estimated the sensitivity to PWV at these frequencies to be approximately 30 times higher than at the frequencies of the MWR. To assess the sensitivity to LWP, three months of radiosonde data (clear and cloudy) were used to compute brightness temperatures. Since the radiosondes do not measure liquid water, differences between model and measurements were attributed to the presence of LWP. In Fig. 4 is shown the difference between measured and modeled brightness temperatures as a function of LWP retrieved with the MWR. Since the uncertainty in MWR retrievals is about 20 g/m^2, data with LWP < 0.02 mm were considered clear. For comparison, the same difference is shown for brightness temperatures measured by the MWR. The ratio $\Delta Tb/\Delta LWP$, the slope of the linear fit, is an indication of the sensitivity to LWP. In Table 2 the slope is displayed for the two MWR channels and for two of the GVR channels. The 183.3 ± 14 GHz channel has a sensitivity that is about 3.5 times higher than the 31.4 GHz channel of the MWR.

V. Retrieval Algorithm

A non-linear algorithm was used to retrieve LWP and PWV from GVR measurements. The algorithm is a Gauss-Newton method [13] that finds the zeroes of the gradient of the cost function:

$$\mathbf{J} = [\mathbf{y} - \mathbf{F(x)}]^{\mathrm{T}} \mathbf{E}^{-1} [\mathbf{y} - \mathbf{F(x)}] + [\mathbf{x} - \mathbf{x}_{\mathbf{a}}]^{\mathrm{T}} \mathbf{S}_{\mathbf{a}}^{-1} [\mathbf{x} - \mathbf{x}_{\mathbf{a}}] \ . \quad (1)$$

In (1) **x** is a 27-element vector whose first element is LWP and whose remaining 26 levels constitute a relative humidity profile between 0 and 10 km. The '*a priori*' constraint $\mathbf{x_a}$ is computed from one year of radiosonde data with covariance $\mathbf{S_a}$. The vector of computed brightness temperatures is **F(x)** and **y** is the vector of the measurements with error covariance **E**. The minimization is achieved by successive iterations starting from a first guess profile of temperature and relative humidity. The first guess profiles are retrieved by linear statistical regression from measurements collected by the 12-channel microwave profiler (MWRP) [12]. The criteria for convergence is that the difference between two successive estimations be smaller than a predetermined threshold: $x_{n+1}(1) - x_n(1) < 0.005$ mm and $x_{n+1}(i) - x_n(i) < 20\%$ for i = 2,27. Upon convergence the algorithm returns the estimated vector $\hat{\mathbf{x}}$ and its error covariance $\mathbf{S_x}$. The post-measurements covariance matrix $\mathbf{S_x}$ is defined as

$$\mathbf{S_x} = (\mathbf{K}^{\mathrm{T}} \mathbf{E}^{-1} \mathbf{K} + \mathbf{S_a}^{-1})^{-1}, \quad (2)$$

where **K** is the Jacobian $K_{ij}=\partial f_i(x)/\partial x_j|_{\mathbf{x=xn}}$ and the superscript "**T**" indicates the transpose matrix. The matrix $\mathbf{S_x}$ is an indication of how well the retrieval is performing with respect to the climatologic average used as statistical constraint. The square roots of its diagonal elements are the standard deviation of the retrieval at each layer. In Fig. 5 an example of $\sqrt{S_x(i,i)}$ is shown together with $\sqrt{S_a(i,i)}$, the prior standard deviation. In the region where the measurements are not contributing to the retrieval the standard deviation tends to the *' a priori'*. This is noticeable at the very top and bottom layers. Where the measurements are contributing the post-measurement standard deviation is smaller than the prior. Contributing factors to the

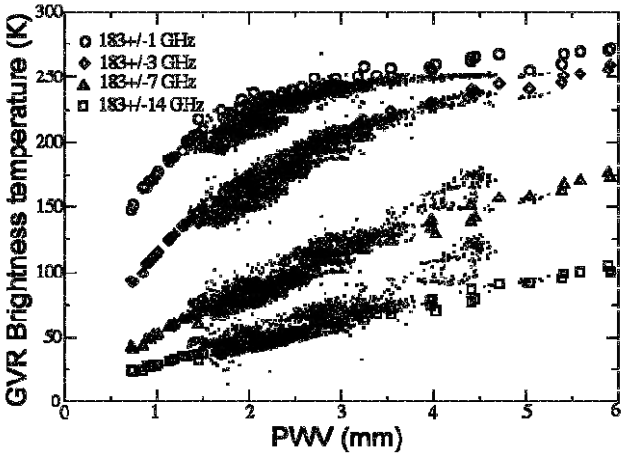

Fig. 3. GVR-measured brightness temperatures as a function of PWV retrieved from the collocated MWR. Data are for non-cloudy conditions only. The circles, diamonds, triangles, and squares are model computations from one year of radiosonde data. The non-linear response to PWV is evisent in the ± 1 and ± 3 channels.

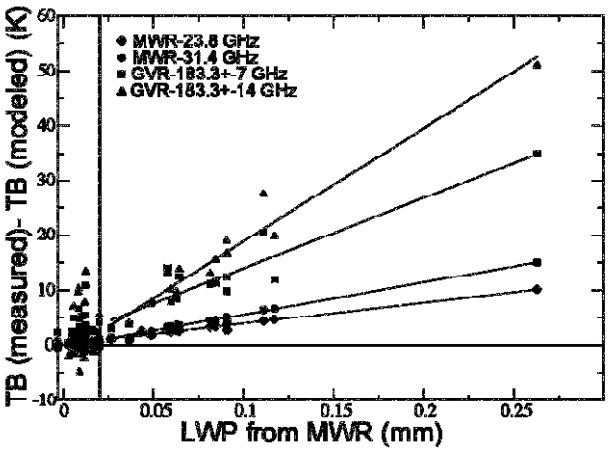

Fig. 4. Sensitivity of GVR-measured brightness temperatures to LWP. The LWP on the x- axis is retrieved from the co-located MWR.

total retrieval covariance are measurement noise, forward model errors and errors deriving by the use of a low-resolution atmospheric profile. In addition, any error in the instrument calibration will appear as a bias in the final result. Calibration may be affected by the thermal stability of the warm target. The estimated calibration accuracy for the instrument is in the range of 1 K. The retrieved relative humidity vector is first converted to specific humidity and then integrated to obtain PWV. The retrieved PWV error covariance is estimated following [13], by applying a linear transformation **h** to $\mathbf{S_x}$:

$$s_{PWV} = \mathbf{h}^{\mathbf{T}} \mathbf{S_x} \mathbf{h}, \tag{3}$$

and the retrieval standard deviation is

$$\varepsilon_{PWV} = \sqrt{s_{PWV}}\,. \tag{4}$$

VI. Retrieval Results

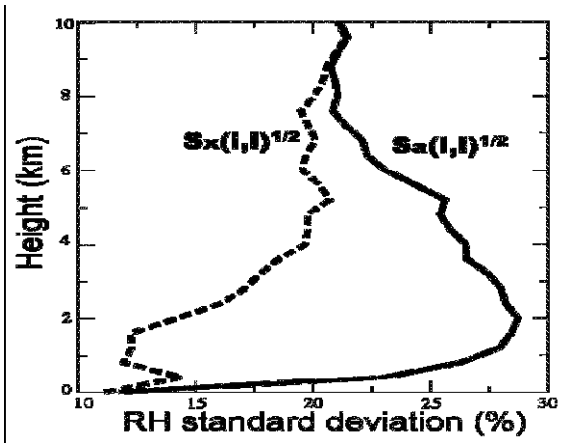

Fig. 5. An example of standard deviation for a relative humidity (RH) profile. The solid line is the prior standard deviation. Where measurements are not contributing to the retrieval the post-measurement covariance is the same as the prior.

A time-series of retrieved PWV and LWP for January 2006 is shown in Fig. 6. Data were collected during prevailing low-humidity conditions. GVR retrievals have the same time resolution (5 minutes) as the MWRP retrievals used to initialize the algorithm. The temporal resolution is therefore 5 minutes. The top panel is the retrieved LWP, while the middle pane is the retrieved PWV. In the bottom panel infrared temperature measured by a Wintronics KT-19.85 infrared thermometer located at the site is shown. When the measured temperature is 223 K, the sky can be considered free of liquid clouds. On the two top panels the solid and dashed lines are the GVR and MWR retrievals respectively. The MWR retrievals are based on an 'a priori' linear statistical retrieval trained with several years of in-situ radiosonde measurements. A Gaussian noise with a standard deviation of 0.5 K is used to simulate a real instrument noise. The radiative transfer model MonoRTM is used in both retrievals. In the non-linear physical algorithm for the GVR, the liquid water layer is added between 0 and 1 km. The first noticeable feature of the comparison is that the GVR retrieves less LWP than the MWR. This is generally true during clear-sky conditions, as it will be shown later, however it is also true under cloudy conditions. In the absence of additional LWP measurements it is difficult to assess the accuracy of the LWP retrievals. The theoretical LWP accuracy computed from (4) (not shown here) varies linearly between 0.004 and 0.012 mm as a function of PWV while the difference between MWR-retrieved and GVR-retrieved LWP increases linearly with the LWP. Although previous studies have shown that MWR retrievals of liquid water may be too high at times, it is not excluded that the differences in the retrievals may be due to issues in the iterative retrievals used for the GVR. Additional investigation is needed to clarify this point, especially on the role of the prior information and statistical constraints. The PWV retrievals from the two instruments are in satisfactory agreement. When the PWV is very low (PWV < 4 mm) it appears that the GVR retrieves less PWV. In Fig. 7 is shown a scatter plot of MWR and GVR-retrieved PWV for cloudy and clear-sky cases during two weeks in December 2005 and two weeks in January 2006. The scatter plot confirms that the PWV from the MWR is slightly higher when the PWV amount is less than 4 mm. In Fig. 8 is shown that the PWV error percentage as estimated from (4), varies approximately between 2 and 4.5% for a range of retrieved PWV between 1.5 and 7.5 mm. In Fig. 9 is shown a comparison of retrieved PWV with measurements from Vaisala R90 radiosondes during the months of November, December and January for clear-sky cases only. Vaisala RS90 radiosonde expected accuracy of relative humidity measurements is estimated at

TABLE II
Slope of Linear Regression Fit

Frequency GHz	Slope ΔTb/ΔLWP (K/mm)
23.8	38.53
31.4	58.71
183.3 ± 7	130.39
183.3 ± 14	205.92

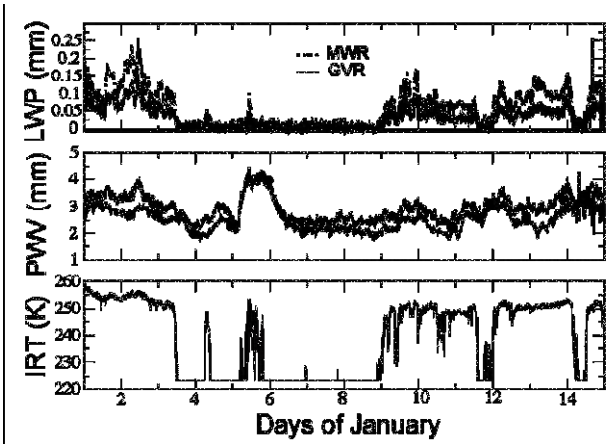

Fig. 6. Time series of PWV and LWP retrieved by the MWR and the GVR in January 2006. The MWR-retrieved parameters are slightly higher than the GVR's. The bottom panel is the infrared temperature measured by the infrared thermometer located on top of the MWRP.

about 5%. This translates in a PWV accuracy of better than 1 mm. The diamonds are the MWR retrievals, empty circles are the GVR retrievals using the MWRP-retrieved profile to initialize the algorithm, and the full circles are GVR retrievals initialized using the radiosonde profiles. For the 41 cases shown in Fig. 8 the MWR slightly overestimated water vapor when radiosonde measurements were below 3 mm. On the other side GVR retrievals display a slight 0.1-mm bias in the other direction. In addition to the total retrieval error defined in (2) and shown in Fig. 8, we examined the influence of the first guess. This was done by running the retrieval in proximity of radiosonde launches and by using the radiosonde profiles, as the first guess, instead than the MWRP-retrieved profiles. The results of this exercise are show in Fig. 9 as black filled circles and they suggest that the uncertainty related to the prior information is not a large source of error. As the PWV amount increases, however, it appears that uncertainties in the prior information have a larger impact on the retrieval. This could be explained by the fact that, as the non-linearity of the retrieval increases, the choice of prior information becomes important for the proper convergence of the algorithm.

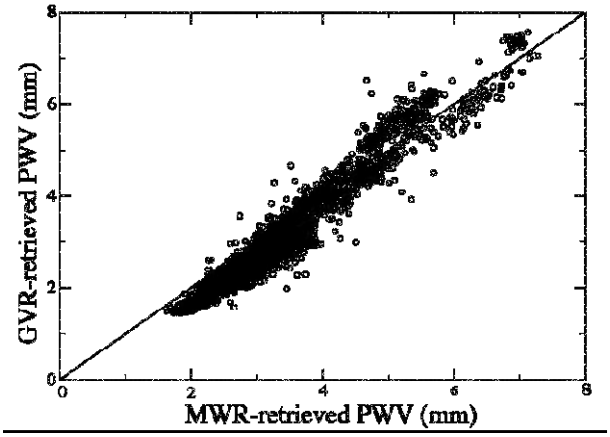

Fig. 7. Scatter plot of MWR-retrieved (x axis) and GVR-retrieved (y axis) PWV (data are from two weeks in December and January).

VII. CLEAR-SKY LWP RETRIEVALS

Tl
in
ur
ab
in
er
ph
du
M
an
an
le
th
be
ur
th
re

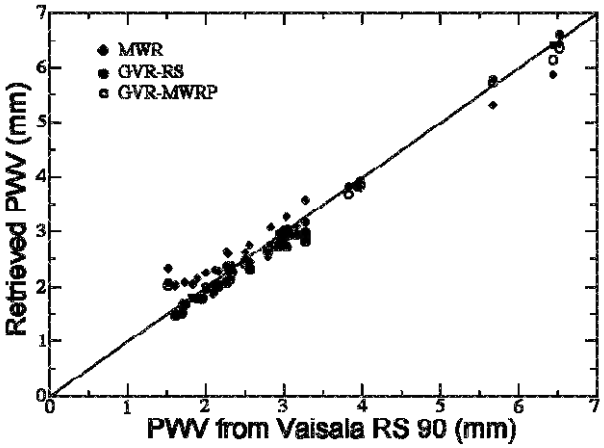

Fig. 9. Comparison of PWV retrieved from the MWR (diamonds) and the GVR(circles) with radiosonde measurements. Data are 41 cases of clear-sky measurements during the months of November, December and January.

water absorption model of [14]. From our studies it emerges that two factors will affect the clear-sky retrievals from the GVR: the modeling of the line absorption (most probably the line width parameter) and uncertainties in brightness temperature measurements. In Table 1 it can be seen that standard deviations of measured-minus-modeled clear sky brightness temperatures are around 3 and 4 K for the 183.3 ± 7 and 183.3 ± 14 GHz channel respectively. From the sensitivity study (see Table 2) it can be estimated that the corresponding uncertainty in the GVR-retrieved LWP can be as large as 0.02 mm in a worst-case scenario. Fig. 10 shows the retrieved LWP distribution for 500 clear-sky cases in January 2006. On the left panel are the MWR retrievals and on the right panel are the GVR retrievals. The mean (0.004 mm) and standard deviation (0.002 mm) for the LWP retrieved from the GVR suggest that the calibration accuracy for the 183.3 ± 7 and ± 14 GHz channel is better than 1 K. This was recently confirmed by an independent calibration that was performed on site with an improved thermal stabilization of the target. Assuming a stable calibration, we can say that the remaining uncertainty is

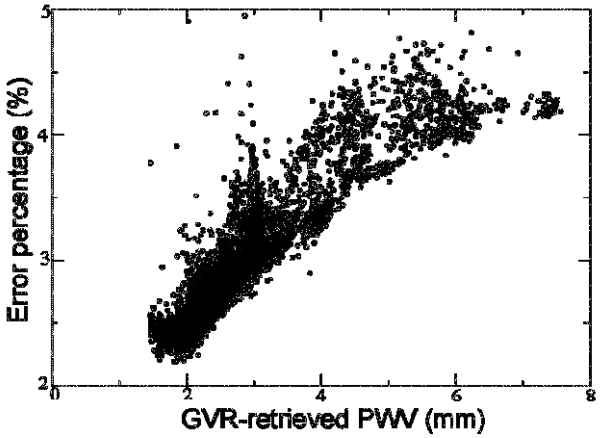

Fig. 8. Estimated error percentage of GVR-retrieved PWV as a function of PWV.

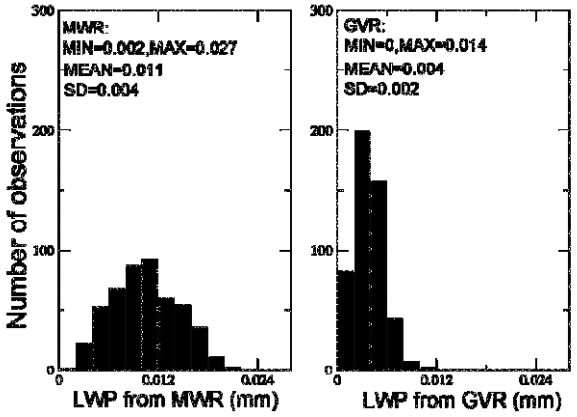

Fig. 10. Clear-sky LWP distributions retrieved by the MWR (left panel) and the GVR (right panel). N= 499 cases in January 2006.

related to the line modeling. On the other side, the MWR retrievals display the larger liquid amount already discussed.

VIII. CONCLUSIONS

In this paper we have analyzed an extensive set of measurements from a ground-based 183.3 GHz water vapor radiometer. The instrument was designed with the purpose of improving water vapor and liquid water retrievals that are greatly needed in radiance simulations and climate models. This is the first time such an extensive set of ground-based data has been available at these frequencies. It has enabled us to assess quality of calibration, the agreement with the model and the retrieval performance. From the analysis it appears that the quality of calibration was very good for the ± 7 and ±14-GHz channels. There may be the need for improved calibration improvement at 183.3 ± 1 and ± 3 GHz, but the error in the brightness temperature at this moment should not be larger than 2 K. Clear-sky model comparisons with MonoRTM simulations were satisfactory.

A retrieval algorithm was developed for PWV and LWP and results were compared with the collocated MWR retrievals and with radiosonde measurements. The GVR generally retrieves less LWP than the MWR and the differences between the two instruments increase at larger LWP amounts. The origin for the discrepancy is not clear and is uner investigation. Retrieved PWV from the two instruments are in good agreement. The GVR retrieves less PWV than the MWR during very dry conditions and it agrees better with radiosonde soundings. Retrieval errors have been estimated to be below 5% when the PWV is in the range of 1 to 8 mm. The effect of the first-guess profile in the retrieval can have some influence when the PWV is higher than 4 mm. In general, given the nonlinear nature of the problem a reasonably close ‘ a priori’ and first-guess profile are important. The estimated LWP error is of 0.006 mm but it could reach 0.02 mm. Clear-sky LWP retrievals show that the main source of error is due to the modeling of the absorption line, but a stable calibration with uncertainties of less than 1 K is essential for good retrievals.

REFERENCES

[1] R. Marchand et al. G. O. Young, “An assessment of microwave absorption models and retrievals of cloud liquid water using clear-sky data,” *J. Geophys. Res.*, vol. 108, no. D24, Dec. 2003.

[2] S. Crewell and U. Löhnert, “Accuracy of cloud liquid water path from ground-based microwave radiometry 2. Sensor accuracy and synergy,” *Radio Sci.*, vol. 38, no. 3, pp. 8042-8052, 2003.

[3] E. R. Westwater, Y. Han, M. D. Shupe, S. Y. Matrosov, “Analysis of integrated cloud liquid and precipitable water vapor retrievals from microwave radiometers during the Heat Budget of the Arctic Ocean project,” *J. Geophys. Res.*, vol. 106, no. D23, pp. 32,019-32,030, 2001.

[4] P. E. Racette, et al., “Measurements of low amounts of precipitable water vapor using ground-based millimeterwave radiometry,” *J. Atmos. Oceanic Technol.*, vol. 22, no. 4, pp. 317-333, Apr. 2005.

[5] R. Lutz, T. T. Wilheit, J. R. Wang, and R. K. Kakar, “Retrieval of atmospheric water-vapor profiles using radiometric measurements at 183 and 90 GHz,” *IEEE Trans. Geosci. Remote Sens.*, vol. 29, no. 4, pp. 602-609, July 1991.

[6] J. R. Wang, P. Racette, M. E. Triesky, W. Manning, “Retrievals of column water vapor using millimeter-wave radiometric measurements,” *IEEE Trans. Geosci. Remote Sens.*, vol. 40, no. 6, pp. 1220-1229, June 2002.

[7] A. Siegenthaler, O. Lezeaux, D. G. Feist, N. Kampfer, “First water vapor measurements at 183 GHz from the high alpine station Jungfraujoch,” *IEEE Trans. Geosci. Remote Sens.*, vol. 39, no. 9, pp. 2084-2086, Sept. 2001.

[8] A. L. Pazmany, “An operational G-band (183 GHz) water vapor radiometer (Submitted),” *Proc. 9th Specialist Meeting on Microwave and Remote Sensing Applications,* San Juan, Puerto Rico, Feb. 28-March 8, 2006.

[9] S.A. Boubakara, S.A. Clough, and R.N. Hoffman, “MonoRTM: A monochromatic radiative transfer model for microwave and laser calculations,” *22nd Annual Review of Atmospheric Transmittance Models*, MA, 1999.

[10] L.S. Rothman et al., “The HITRAN 2004 molecular spectroscopic database,” *J. Quant. Spectrosc. Radiat. Transfer,* vol. 96, pp. 139-204, 2005.

[11] S. A. Clough, F. X. Kneizys, and R. W. Davies, “Line shape and the water vapor continuum,” *Atmos. Res.*, vol. 23, pp. 229-241, 1989.

[12] J. C. Liljegren, M. P. Cadeddu, and A. Pazmany, “Retrievals of atmospheric temperature and water vapor profiles in the Arctic (Submitted),” *Proc. 9th Specialist Meeting on Microwave and Remote Sensing Applications,* San Juan, Puerto Rico, Feb. 28-March 8, 2006.

[13] C. D. Rodgers, “Inverse methods for atmospheric sounding. Theory and practice,” World Scientific, pp. 73, 2000.

[14] H. J. Liebe, G. A. Hufford, and T. Manabe, “A model for the complex permittivity of water at frequencies below 1 THz,” *Int. J. Infrared Millimeter Waves*, vol. 12, pp. 659-675, 1991.